Inorganic Chemistry

ARTICLE

pubs.acs.org/IC

Structural Chemistry, Monoclinic-to-Orthorhombic Phase Transition, and CO_2 Adsorption Behavior of the Small Pore Scandium Terephthalate, $Sc_2(O_2CC_6H_4CO_2)_3$, and Its Nitro- And Amino-Functionalized Derivatives

John P. S. Mowat,[†] Stuart R. Miller,[‡] John M. Griffin,[†] Valerie R. Seymour,[†] Sharon E. Ashbrook,[†] Stephen P. Thompson,[§] David Fairen-Jimenez,[∥] Ana-Maria Banu,[∥] Tina Düren,[∥] and Paul A. Wright*[,†]

[†]EaStCHEM School of Chemistry, University of St. Andrews, United Kingdom

[‡]Institut Lavoisier, 45, Avenue des Etats-Unis, Université de Versailles St-Quentin en Yvelines, Versailles, France

[§]Diamond Light Source, Harwell Science and Innovation Campus, Didcot, Oxfordshire OX11 0DE, United Kingdom

[∥]Institute for Materials and Processes, School of Engineering, The University of Edinburgh, United Kingdom

Supporting Information

ABSTRACT:

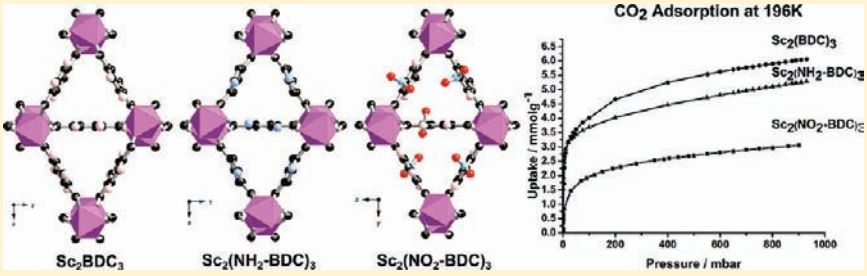

The crystal structure of the small pore scandium terephthalate $Sc_2(O_2CC_6H_4CO_2)_3$ (hereafter Sc_2BDC_3, BDC = 1,4-benzenedicarboxylate) has been investigated as a function of temperature and of functionalization, and its performance as an adsorbent for CO_2 has been examined. The structure of Sc_2BDC_3 has been followed in vacuo over the temperature range 140 to 523 K by high resolution synchrotron X-ray powder diffraction, revealing a phase change at 225 K from monoclinic $C2/c$ (low temperature) to *Fddd* (high temperature). The orthorhombic form shows negative thermal expansivity of 2.4×10^{-5} K^{-1}: Rietveld analysis shows that this results largely from a decrease in the c axis, which is caused by carboxylate group rotation. ^2H wide-line and MAS NMR of deuterated Sc_2BDC_3 indicates reorientation of phenyl groups via π flips at temperatures above 298 K. The same framework solid has also been prepared using monofunctionalized terephthalate linkers containing -NH_2 and -NO_2 groups. The structure of $Sc_2(NH_2\text{-}BDC)_3$ has been determined by Rietveld analysis of synchrotron powder diffraction at 100 and 298 K and found to be orthorhombic at both temperatures, whereas the structure of $Sc_2(NO_2\text{-}BDC)_3$ has been determined by single crystal diffraction at 298 K and Rietveld analysis of synchrotron powder diffraction at 100, 298, 373, and 473 K and is found to be monoclinic at all temperatures. Partial ordering of functional groups is observed in each structure. CO_2 adsorption at 196 and 273 K indicates that whereas Sc_2BDC_3 has the largest capacity, $Sc_2(NH_2\text{-}BDC)_3$ shows the highest uptake at low partial pressure because of strong -$NH_2 \cdots CO_2$ interactions. Remarkably, $Sc_2(NO_2\text{-}BDC)_3$ adsorbs 2.6 mmol CO_2 g^{-1} at 196 K ($P/P_0 = 0.5$), suggesting that the -NO_2 groups are able to rotate to allow CO_2 molecules to diffuse along the narrow channels.

1. INTRODUCTION

The propensity for porous metal organic frameworks, or MOFs, to show structural flexibility while retaining their framework connectivity is much greater than that of their purely inorganic counterparts, such as zeolites and zeotypes. There are many examples of such solids that show very pronounced "breathing" effects in response to changes in temperature or adsorbate pressure. Among these, the metal terephthalates MIL-53[1] and MIL-88[2] exhibit particularly large volume changes, resulting from the ability of terephthalate linkers to show hinge-like motion where they coordinate in bridging mode to the metal cations (terephthalate = 1,4-benzenedicarboxylate = BDC). This results in very large volume expansions (up to 125% for MIL-88B(Cr))[3] as well as symmetry changes, and the nature of the structural change depends on the type and partial pressure of adsorbate. Not all terephthalate-based MOFs are flexible in this way, however. The prototypical zinc terephthalate MOF-5,

Received: June 29, 2011
Published: September 29, 2011

Table 1. Details of Hydrothermal and Solvothermal Syntheses of Sc_2BDC_3 and Functionalized Analogues Prepared in This Study[a]

				molar ratio				
temp./K	solvent	scandium source	ligand	Sc	L	solvent	time/h	product
493	DEF	$Sc(NO_3)_3{\cdot}3H_2O$	BDC	1	1.5	300	72	Sc_2BDC_3
493	DEF	$Sc(NO_3)_3{\cdot}3H_2O$	d_4-BDC	1	1.5	600	72	$Sc_2(d_4\text{-BDC})_3$
493	H_2O	Sc_2O_3	BDC	1	1.5	600	72	$Sc_2BDC_3 + Sc_2O_3$
463	DEF	$Sc(NO_3)_3{\cdot}3H_2O$	NH_2-BDC	1	1.5	300	72	MIL-88(Sc)-NH_2
463	DEF	$Sc(NO_3)_3{\cdot}3H_2O$	NO_2-BDC	1	1.5	300	72	MIL-53(Sc)-NO_2
463	H_2O	$Sc(NO_3)_3{\cdot}3H_2O$	NH_2-BDC	1	1.5	600	72	MIL-88(Sc)-NH_2
463	H_2O	$Sc(NO_3)_3{\cdot}3H_2O$	NO_2-BDC	1	1.5	600	72	$Sc_2(NO_2\text{-BDC})_3$
463	H_2O	Sc_2O_3	NH_2-BDC	1	1.5	600	72	$Sc_2(NH_2\text{-BDC})_3 + Sc_2O_3$
463	H_2O	Sc_2O_3	NO_2-BDC	1	1.5	600	72	$Sc_2(NO_2\text{-BDC})_3 + Sc_2O_3$

[a] BDC = terephthalic acid, NO_2- and NH_2-BDC are the monofunctionalized nitro- and amino-terephthalic acids; DEF = diethylformamide.

for example, is more rigid, with smaller volume changes measured upon adsorption of molecules.[4,5] Nevertheless, variable temperature diffraction reveals strong linear negative expansion behavior,[6,7] and the analysis of dynamics using variable temperature ^2H NMR indicates that the phenyl groups exhibit π flips that increase in rate with temperature with an activation energy of 11.3 ± 2.0 kcal/mol.[5,7] Similar motion of the phenyl rings is observed in MIL-53 and MIL-47.[8] The structural response of terephthalate MOFs to variation in temperature or adsorbate pressure (or more strictly, chemical potential) will determine the selectivity and capacity of their adsorption. In addition, the motion of the phenyl groups will modify the effective pore size between rings if it enables pores to open up. For this reason, it is important to measure and understand both changes in their crystal structures (their flexibility) and also the motion of their terephthalate linkers (their dynamics) as a response to temperature.

Furthermore, it is known that for many structures it is possible to include functionalized terephthalates into the structure in place of the unfunctionalized dicarboxylate, and that this modifies their structural and adsorptive properties. For MIL-53(Fe) for example[9] a series of functionalized terephthalates (-Cl, -Br, -CF_3, -CH_3, -NH_2, -OH, -CO_2H) with varying polarity, hydrophobicity, and acidity were used in the synthesis of MIL-53(Fe)-type materials to modify the pore surface systematically while maintaining the flexibility.

The scandium terephthalate Sc_2BDC_3 is a small pore MOF with openings about 3 Å in free diameter (calculated crystallographic pore size distribution indicates a range of pore sizes from 2.5−3.25 Å) that shows remarkable thermal stability and hydrophobicity and is able to adsorb a range of small gas molecules.[10] In situ single-crystal X-ray diffraction studies at 230−235 K in the presence of CO_2, CH_4, and C_2H_6 gases were able to locate the favored sites of physisorption of these molecules within the channels.[10] These measurements showed that the structure could take either monoclinic or orthorhombic crystal forms, depending on the gas in contact with the crystals. Here we investigate the structural response of Sc_2BDC_3 to variations of temperature in vacuo, by synchrotron powder X-ray diffraction, and observe the monoclinic-orthorhombic phase transition and the negative thermal expansivity of the higher temperature orthorhombic phase. Furthermore, we have measured the motion of the phenyl groups as the temperature is increased. The observed adsorption behavior of CO_2 on Sc_2BDC_3 is interpreted via molecular modeling in the light of the structural data.

Despite the high density of terephthalate linkers within Sc_2BDC_3, which result in its small pore character, it is possible to prepare the MOF with monofunctionalized ligands of the form $O_2CC_6H_3XCO_2$, where X is NH_2 or NO_2. The influence of the incorporation of these monofunctionalized terephthalates on the crystal symmetry and structure of Sc_2BDC_3 has been determined at 100 and 298 K (and higher temperatures for the nitro-functionalized solid). In addition, the effect of inclusion of the functional groups on the adsorption of CO_2 up to 1 bar pressure has been measured at 196 and 273 K, temperatures chosen to determine maximum uptake and strength of interaction of CO_2 with the adsorbents. The results indicate that the presence of functional groups can stabilize one or other of the crystal forms of Sc_2BDC_3 and that partial ordering of groups on particular crystallographic carbon atom positions can result. Furthermore, CO_2 adsorption studies suggest that motion of -NO_2 groups can occur, even at low temperatures, and that the heat of CO_2 adsorption can be increased by incorporating NH_2 groups.

2. EXPERIMENTAL SECTION

2.1. Synthesis, Characterization, and Adsorption. Syntheses were performed using either scandium oxide (Sc_2O_3, 99.999%, Stanford Materials Corporation) or scandium nitrate ($Sc(NO_3)_3{\cdot}3H_2O$, 99.9%, Metall Rare Earth Limited) as the scandium source. Sc_2BDC_3 was prepared according to the literature solvothermal method:[10] terephthalic acid (1,4-benzenedicarboxylic acid, H_2BDC, Aldrich, 98%, 0.539 mmol, 0.0895 g) and scandium nitrate (0.269 mmol, 0.0768 g) in the ratio 2:1 were dissolved in diethylformamide, DEF (Alfa Aesar, 98%, 6 mL) and heated at 463 K for 72 h. The resulting solid was washed with ethanol and dried at 333 K. A deuterated sample of Sc_2BDC_3 was prepared for variable temperature ^2H solid-state NMR via the same reported solvothermal route using d_4-terephthalic acid (Sigma, 98 atom % D).

Hydrothermal crystallization using scandium oxide, reported to produce the Sc_2BDC_3 framework,[11] was successful for the preparation of the functionalized forms of the Sc_2BDC_3 material using the 2-nitroterephthalic acid (Alfa Aesar, 99%) and 2-aminoterephthalic acid (Aldrich, 99%). Subsequently, hydrothermal synthesis using scandium nitrate was also successful in attempts to prepare the -NO_2 form of Sc_2BDC_3 (Table 1).

As-synthesized materials were identified by means of powder X-ray diffraction, thermo-gravimetric analysis (TGA), and chemical analysis. Laboratory X-ray diffraction patterns were obtained in Debye−Scherrer geometry within sealed 0.7 mm quartz capillaries on a Stoe STADI/P diffractometer with monochromated Cu $K_{\alpha 1}$ X-rays (λ = 1.54056 Å).

dx.doi.org/10.1021/ic201387d |Inorg. Chem. 2011, 50, 10844–10858

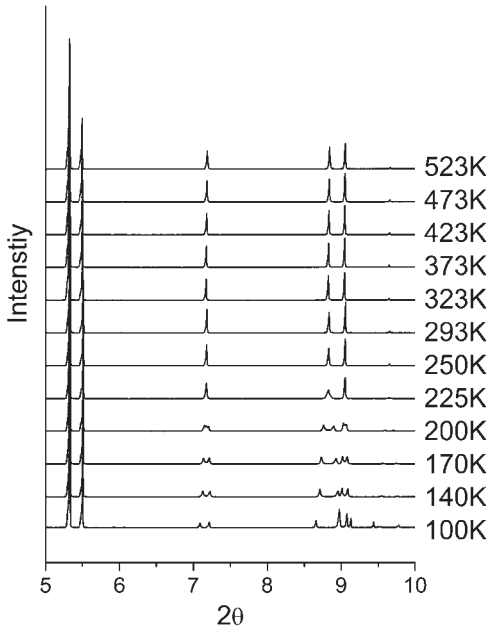

Figure 1. Variable temperature synchrotron powder X-ray data for Sc_2BDC_3 from 100 to 523 K (plotted for the range 5−10° 2θ) showing the symmetry change from monoclinic (low temperature form) to orthorhombic (high temperature form).

Initial phase identification to confirm purity was possible by direct comparison of observed diffraction patterns with the literature example of Sc_2BDC_3.[10]

Synchrotron X-ray diffraction data were obtained at the high resolution powder diffraction beamline I11 at the Diamond Light Source.[12] Samples were ground fine to avoid preferential orientation and activated in quartz glass capillaries under vacuum and flame-sealed before investigation to ensure the thermal behavior was independent of adsorbed guest species. Samples were activated at 623 K for the pure terephthalate and 443 K for the functionalized materials. Data was collected between 100 and 523 K for Sc_2BDC_3, at 100 K for $Sc_2(NH_2\text{-}BDC)_3$, and at 100, 373, and 473 K for $Sc_2(NO_2\text{-}BDC)_3$ (looking to see if a phase transition existed). The temperature was controlled by means of a Cryostream 700 Series between 100 and 293 K and using a hot air blower in the region above room temperature 293 K−523 K. In each case the diffraction pattern was collected from 0 to 140° 2θ by constant velocity scanning in Debye−Scherrer geometry using the beamline's multianalyzer crystal system, with the measured intensities binned to a 2θ interval of 0.001°. In addition, laboratory diffraction was performed on the same samples at 298 K, and single crystal diffraction was performed at 298 K on suitable crystals of $Sc_2(NO_2\text{-}BDC)_3$ prepared hydrothermally with $Sc(NO_3)_3$.

TGA was performed at 5 K min^{-1} up to 1172 K under flowing air. Elemental analysis (carbon, hydrogen, nitrogen) was performed on pure samples using a Carlo Erba instruments EA 1110 CHNS analyzer.

Solid-state NMR experiments were performed using Bruker Avance III spectrometers operating at magnetic field strengths of 9.4 and 14.1 T. Experiments at both magnetic fields were carried out using Bruker 4-mm MAS probes. Chemical shifts are given relative to TMS for ^{13}C and ^{2}H, and 0.2 M $ScCl_3$ (aq) for ^{45}Sc. ^{13}C transverse magnetization was obtained by ramped cross-polarization (CP) from ^{1}H. Two-pulse phase modulation (TPPM) ^{1}H decoupling was applied during acquisition. ^{13}C CP MAS NMR spectra were acquired with between 4400 and 6144 transients separated by a recycle interval of 3 s. ^{45}Sc MAS NMR spectra were obtained by direct polarization of ^{45}Sc, using between 256 and 1024 transients separated by a recycle interval of 3 s. Variable-temperature ^{2}H wide-line NMR spectra were acquired for a static sample in the range 298−383 K using the quadrupolar echo pulse sequence ($90°_{\varphi}-\tau-90°_{\varphi'}-\tau$). Spectra were recorded using an echo duration, τ, of 40 μs and a 16-step phase cycle designed to refocus both linear and quadratic spin interactions.[13] Spectra were obtained using between 2206 and 14336 transients separated by a recycle interval of 5 s. Further experimental details are given in the figure captions.

Adsorption isotherms of N_2 on all samples were measured at 77 K using a Micromeritics Tristar II 3020. Adsorption of CO_2 was measured on Sc_2BDC_3 prepared solvothermally and on functionalized samples prepared hydrothermally using scandium oxide as the scandium source. Isotherms were collected up to 900 mbar at 196 K (ethanol/dry ice mixture) and 273 K (Grant GR150 thermostatic refrigerated bath) using a Hiden IGA automatic gravimetric porosimeter. Prior to adsorption of N_2 or CO_2, the samples were heated at 443 K under a vacuum of 3×10^{-7} mbar for 8 h. In addition, laboratory powder X-ray diffraction was performed on samples in quartz glass capillaries that had been activated at 443 K and allowed to adsorb CO_2 at 298 K and 1 bar before being sealed (by glue).

2.2. Crystallography. For structural studies by powder X-ray diffraction, samples of Sc_2BDC_3 prepared solvothermally were used because they were the most crystalline. The functionalized samples examined were those prepared hydrothermally using scandium oxide as the scandium source. High resolution synchrotron powder diffraction data obtained at DLS I11 on the pure terephthalate form of Sc_2BDC_3 over the temperature range 100−523 K (Figure 1) was of suitable quality for Rietveld refinement[14,15] using starting models (monoclinic *C*2/*c* at 100 K−200 K or orthorhombic *Fddd* at 225 K−523 K) from reported single-crystal X-ray diffraction studies.[10] There were no guest species present as the samples had been heated under vacuum and sealed prior to analysis. In each case, initial Le Bail[16] fitting of the cell parameters in the relevant symmetry indicated good agreement to the literature structures for Sc_2BDC_3. Following this, Rietveld analysis was used to obtain the final atomic positions at each temperature. Bond restraints were applied (Sc−O, 2.09(2) Å; O−O, 2.97(2) Å; O−C, 1.27(2) Å; aromatic C−C, 1.39(2); aromatic-carboxylate C−C, 1.49(2) Å). Examples of Rietveld plots for the orthorhombic and monoclinic forms are given in Figures 2a and 2b and full structural data are given in Table 2 and the Supporting Information.

For the functionalized materials $Sc_2(NH_2\text{-}BDC)_3$ and $Sc_2(NO_2\text{-}BDC)_3$ the low temperature structure (100 K) was solved from high-resolution synchrotron powder diffraction data from I11. Initial unit cell determination from the observed diffraction patterns, using the DICVOL04 program in the Fullprof suite of programs,[17] determined which of the literature structural models (orthorhombic *Fddd* (observed for the -NH_2 form) or monoclinic *C*2/*c* (observed for the NO_2-form) was appropriate. Following this, a framework model was chosen from published structural models derived from single crystal studies on the pure terephthalate Sc_2BDC_3[10] and this was used as a starting model in Rietveld refinement. Atomic positions for the functional groups were identified by difference Fourier mapping and confirmed by geometrically placing atoms in all the possible crystallographic sites and allowing the occupancy to refine (where the sum of the occupancy of the sites was constrained to total one group per phenyl ring). The Rietveld plots for $Sc_2(NH_2\text{-}BDC)_3$ and $Sc_2(NO_2\text{-}BDC)_3$ at 100 K are given in Figures 3a and b, and refined cell parameters and crystallographic data are given in Table 3 and in the Supporting Information. In the case of the $Sc_2(NH_2\text{-}BDC)_3$ some unreacted scandium oxide was observed as a second phase, and the peaks were fitted via a two-phase Rietveld refinement.

For the orthorhombic $Sc_2(NH_2\text{-}BDC)_3$ at 100 K there are two crystallographically different terephthalate linkers, and three crystallographically different carbon sites possible for the amine group, for each of which there are either two or four symmetrically equivalent positions. The difference Fourier technique was successful in locating groups in two of the three crystallographically distinct sites (with statistical

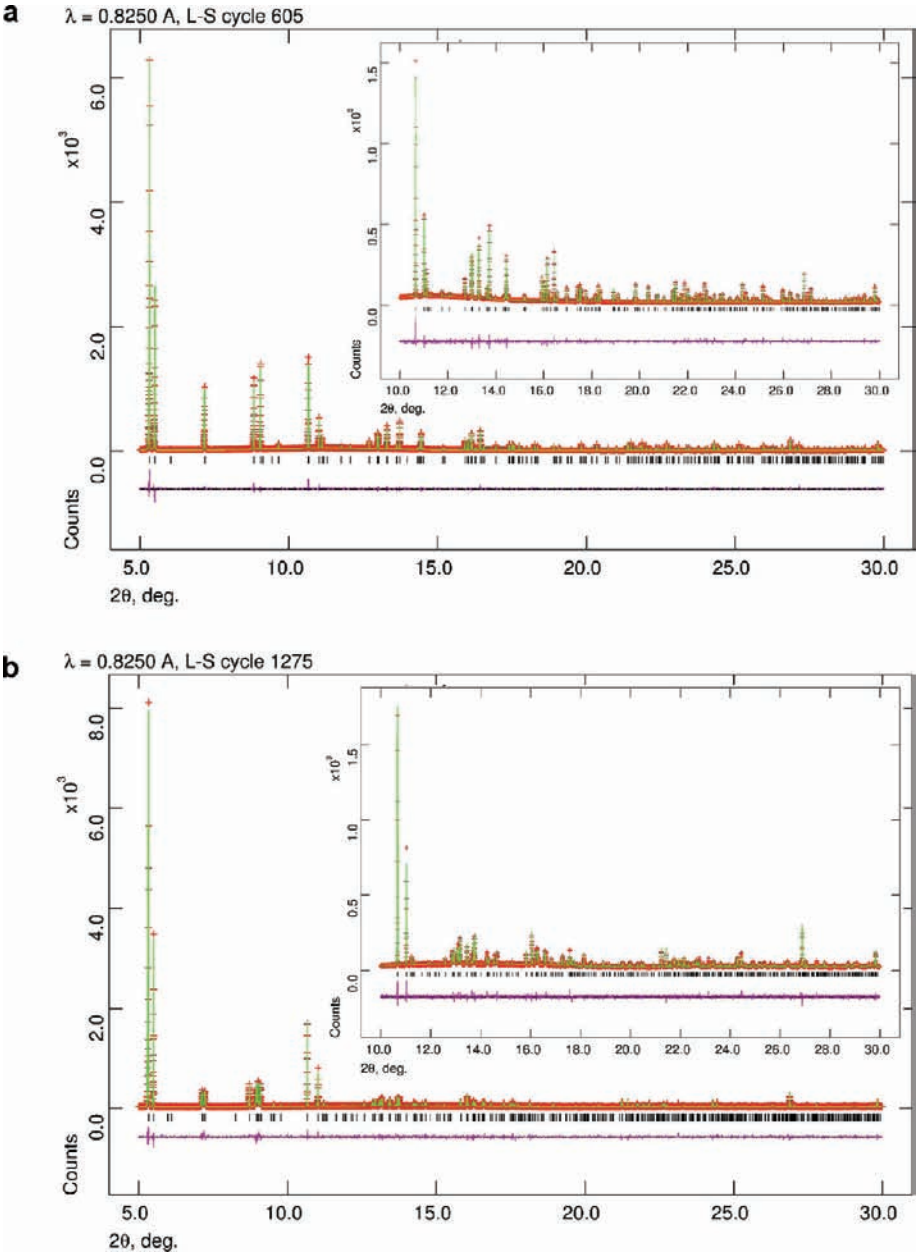

Figure 2. Rietveld profile fits to synchrotron powder X-ray data for Sc_2BDC_3 in (a) the orthorhombic form at 373 K and (b) in the monoclinic form at 140 K, in each case preheated and sealed and examined under vacuum (Experimental data, red markers; fitted profile, green; difference purple.).

disorder over symmetry-related positions). To verify this, amino groups in all possible crystallographic sites were positioned geometrically, and the occupancy of the sites was allowed to vary with the constraint that the sum of the occupancies in all sites was equivalent to one group per aromatic ring. This confirmed that two out of the three sites were occupied. This model was successfully used as a starting point for refinement of the structure at 298 K, which remained in the orthorhombic space group (Table 3).

For the monoclinic $Sc_2(NO_2\text{-}BDC)_3$ there are six possible crystallographically distinct carbon sites for -NO_2 groups. Initial difference Fourier mapping gave some of the positions, but a combined approach using geometric positioning and constrained-occupancy refinement was used to determine the final structure at 100 K. The structure was found to remain monoclinic upon raising the temperature to 473 K, and could be refined using the low temperature structure as a starting point in all cases (See Table 3 and Supporting Information). Further evidence for the position of the -NO_2 group was obtained by single-crystal diffraction on a sample of the $Sc_2(NO_2\text{-}BDC)_3$ prepared hydrothermally using scandium nitrate (Table 1). Data were collected using a Rigaku Mo MM007 high brilliance generator and Saturn 70 CCD detector, at least a full hemisphere of data was collected using ω scans, and intensities were corrected for Lorentz-polarization and for absorption. The data collection was at room temperature. The structure was solved using direct methods, and hydrogen atoms were fixed in idealized positions. The data was refined using the SHELX suite of programs to give a final structural model ($C2/c$, a = 8.669(4) Å, b = 34.370(15) Å, c = 11.053(6) Å, β = 110.486(6)°. R_I = 0.157: see Supporting Information for details).[18] The single-crystal structure is closely similar to that obtained from Rietveld analysis of the synchrotron powder X-ray data on the bulk phase sample.

dx.doi.org/10.1021/ic201387d |*Inorg. Chem.* 2011, 50, 10844–10858

Table 2. Crystallographic Details of Sc_2BDC_3 As a Function of Temperature, As Determined from Synchrotron Powder X-ray data

structure	Sc_2BDC_3 −140 K	Sc_2BDC_3 −170 K	Sc_2BDC_3 −250 K	Sc_2BDC_3 −293 K	Sc_2BDC_3 −323 K	Sc_2BDC_3 −373 K	Sc_2BDC_3 −423 K	Sc_2BDC_3 −473 K	Sc_2BDC_3 −523 K
formula unit	$Sc_2(C_8H_4O_4)_3$	$Sc_2(C_8H_4O_4)_3$	$Sc_2(C_8H_4O_4)_3$	$Sc_2(C_8H_4O_4)_3$	$Sc_2(C_8H_4O_4)_3$	$Sc_2(C_8H_4O_4)_3$	$Sc_2(C_8H_4O_4)_3$	$Sc_2(C_8H_4O_4)_3$	$Sc_2(C_8H_4O_4)_3$
formula weight	582.26	582.26	582.26	582.26	582.26	582.26	582.26	582.26	582.26
temperature/K	140	170	250	293	323	373	423	473	523
space group	*C*2/*c*	*C*2/*c*	*Fddd*	*Fddd*	*Fddd*	*Fddd*	*Fddd*	*Fddd*	*Fddd*
X-ray source	synchrotron	synchrotron	synchrotron	synchrotron	synchrotron	synchrotron	synchrotron	synchrotron	synchrotron
diffractometer	beamline I11	beamline I11	beamline I11	beamline I11	beamline I11	beamline I11	beamline I11	beamline I11	beamline I11
wavelength (Å)	0.826019	0.826019	0.826019	0.825028	0.825028	0.825028	0.825028	0.825028	0.825028
unit cell (Å)									
a/Å	8.75434(14)	8.75468(15)	8.75292(4)	8.745851(13)	8.742107(14)	8.73461(15)	8.72548(2)	8.71576(2)	8.704711(3)
b/Å	34.38536(13)	34.37449(16)	20.7551(5)	20.74388(3)	20.739628(3)	20.733114(3)	20.728004(2)	20.722986(3)	20.71887(3)
c/Å	11.14542(8)	11.16967(1)	34.35779(8)	34.34896(4)	34.34945(4)	34.35274(4)	34.35838(4)	34.36496(4)	34.37361(6)
β/deg	111.4791(8)	111.7476(1)	90	90	90	90	90	90	90
volume/Å^3	3122.00(5)	3122.13(6)	6241.70(4)	6231.68(2)	6227.83(2)	6221.131(14)	6214.124(15)	6206.88(2)	6199.34(3)
no. reflections	404	630	471	665	665	663	661	659	657
no. atoms (non-H)	20	20	11	11	11	11	11	11	11
no. restraints	39	39	22	22	30	30	22	22	22
R	0.0823	0.0864	0.0751	0.046	0.0479	0.0436	0.0434	0.045	0.0488
wR	0.1102	0.1146	0.0969	0.0644	0.0659	0.0607	0.0594	0.0635	0.0693
max. and min residual e- density (e/Å^3)	0.188, −0.254	0.809, −0.528	0.582, −0.641	0.532, −0.425	0.523, −0.554	0.497, −0.498	0.602, −0.516	0.627, −0.447	0.464, −0.439

2.3. Simulation. CO_2 adsorption on three forms of the Sc_2BDC_3 structure observed experimentally was investigated using grand canonical Monte Carlo (GCMC) simulation[19] implemented in the multipurpose simulation code MUSIC.[20] In the grand canonical ensemble, the chemical potential, the volume, and the temperature are kept fixed as in adsorption experiments. Atomistic models were used for the Sc_2BDC_3 structures, with the atoms frozen at the crystallographic positions. In the simulations, CO_2 molecules were randomly moved, rotated, inserted, and deleted, allowing the number of molecules in the framework to fluctuate. The chemical potential was related to the system pressure by the Peng−Robinson equation of state.[21]

The standard 12−6 Lennard-Jones (L-J) potential was used to model the interatomic interactions. The parameters for the framework atoms were obtained from the Dreiding force field,[22] while CO_2 was modeled by the TraPPE three-center model[23] (Supporting Information, Table S3). The Lorentz−Berthelot mixing rules were employed to calculate the mixed parameters. Interactions beyond 15 Å were neglected for the simulations. Mulliken partial charges for the framework atoms were calculated using CASTEP[24] and are given in the Supporting Information. A total number of 5×10^7 Monte Carlo steps were performed. The first 40% were used for system equilibration, carefully ensuring that thermodynamic equilibrium was reached, while the remaining steps were used to calculate the ensemble averages. After equilibration, snapshots were obtained, which represent the position of all CO_2 molecules from a single configuration during the simulation process. Snapshots provide a visual impression about the degree of pore filling and organization of the CO_2 molecules inside the framework, and are reported here for simulations at 235 K (at which temperature the position of CO_2 has been observed experimentally[10]) and a pore filling of 3.5 mmol g^{-1}.

3. RESULTS AND DISCUSSION

3.1. Synthesis and Characterization. Sc_2BDC_3 was prepared solvothermally using diethylformamide (requiring scandium nitrate) or hydrothermally (with either scandium nitrate or scandium oxide) as reported previously. TGA (Supporting Information) and NMR indicated that there was no solvent in the pores, although in some cases there was some admixed unreacted scandium oxide. Using monofunctionalized terephthalic acids, it was possible to prepare materials with the Sc_2BDC_3 framework hydrothermally by reacting the 2-nitro- and 2-aminoterephthalic acids with scandium oxide or scandium nitrate. Under solvothermal conditions, using nitro-terephthalic acid gives MIL-53(Sc)-NO_2 and using amino-terephthalic acid gives MIL-88(Sc)-NH_2 under the conditions examined. Laboratory powder diffraction of the functionalized Sc_2BDC_3 materials prepared hydrothermally (using either scandium oxide or scandium nitrate) indicated that while $Sc_2(NH_2\text{-}BDC)_3$ is orthorhombic at room temperature, $Sc_2(NO_2\text{-}BDC)_3$ is monoclinic (See Supporting Information).

The thermal stability of the functionalized Sc_2BDC_3 forms was measured using TGA analysis under air. The $Sc_2(NH_2\text{-}BDC)_3$ showed no weight loss up to the final decomposition temperature of 700 K after which the residue was Sc_2O_3. From the TGA analysis the presence of Sc_2O_3 impurity was found to be 18%. This was fitted in analysis of the powder X-ray diffraction in a two-phase refinement, and the impurity is taken into consideration when calculating the mass of sample for adsorption experiments. Elemental analysis including the impurity was in reasonable agreement, for $0.82[Sc_2(NH_2\text{-}BDC)_3]\cdot 0.18[Sc_2O_3]$: Expected C 38.5 wt %, N 5.6 wt %, H 1.96 wt %; Measured C 37.7 wt %, N 4.9 wt %, H 1.8 wt %. Thermal analysis of the $Sc_2(NO_2\text{-}BDC)_3$ again showed no weight loss up to its final decomposition

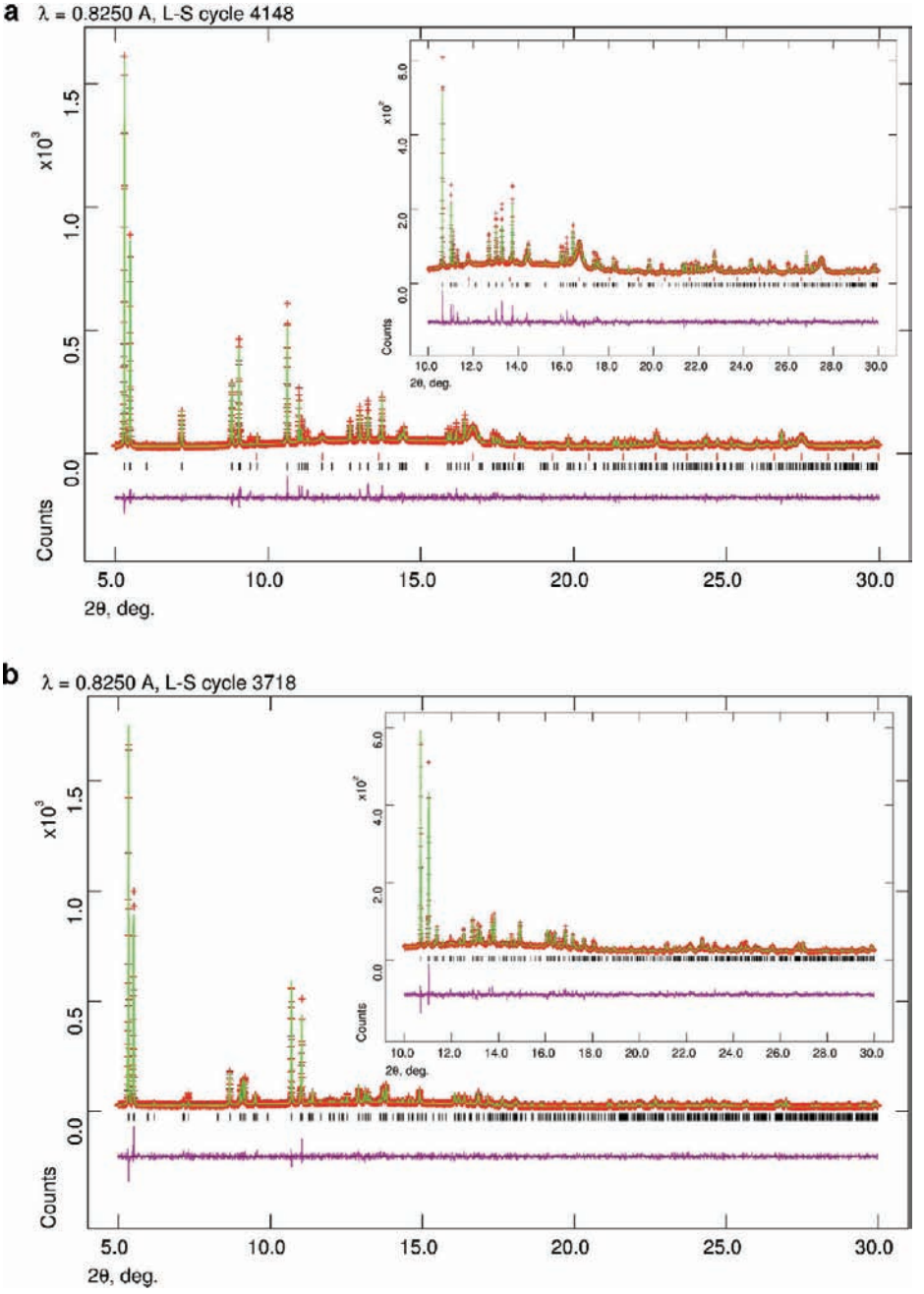

Figure 3. Rietveld profile fits to synchrotron powder X-ray data for functionalized Sc_2BDC_3; (a) $Sc_2(NH_2\text{-}BDC)_3$ with Sc_2O_3 impurity and (b) $Sc_2(NO_2\text{-}BDC)_3$. In each case the samples were preheated and sealed and examined under vacuum at 100 K (Experimental data, red markers; fitted profile, green; difference, purple).

at 680 K to Sc_2O_3. Mass calculations of the TGA suggests some Sc_2O_3 impurity (<5%), as does the elemental analysis, but this was not observed in the X-ray diffraction pattern and was not taken into account for the adsorption experiments. Elemental analysis showed reasonable agreement but suggests some Sc_2O_3 impurity: Expected, C 40.2 wt %, N 5.9 wt %, H 1.3 wt %; Measured, C 36.7 wt %, N 4.9 wt %, H 0.9 wt %.

Room temperature ^{45}Sc (9.4 T) MAS NMR spectra for unfunctionalized and functionalized Sc_2BDC_3 are shown in Figure 4. The spectrum for $Sc_2(BDC)_3$, shown in Figure 4a, exhibits a second-order quadrupolar-broadened MAS line shape corresponding to a single site with a quadrupolar coupling constant, C_Q, of 4.5 MHz and asymmetry parameter, η_Q, of 0.2. This is consistent with the single Sc site in the crystal structure and is in good agreement with previous data reported for the same material.[11] In contrast to Sc_2BDC_3, the ^{45}Sc MAS NMR spectra for the functionalized solids, shown in Figures 4b and 4c, show smooth featureless lineshapes with characteristic "tails" at low frequency, indicating disorder. This can be attributed to statistical disorder of the orientations of the functional groups resulting in a distribution of Sc quadrupolar coupling constants. Despite the disorder, the linewidths for $Sc_2(NH_2\text{-}BDC)_3$ and $Sc_2(NO_2\text{-}BDC)_3$ appear slightly reduced compared with that of $Sc_2(BDC)_3$, indicating a smaller average C_Q for the

dx.doi.org/10.1021/ic201387d |*Inorg. Chem.* 2011, 50, 10844–10858

Table 3. Crystallographic Details of $Sc_2(NO_2\text{-}BDC)_3$ and $Sc_2(NH_2\text{-}BDC)_3$ As a Function of Temperature, As Determined from Synchrotron Powder X-Ray Data

structure	$Sc_2(NO_2\text{-}BDC)_3$-100 K	$Sc_2(NO_2\text{-}BDC)_3$-293 K	$Sc_2(NO_2\text{-}BDC)_3$-373 K	$Sc_2(NO_2\text{-}BDC)_3$-473 K	$Sc_2(NH_2\text{-}BDC)_3$-100 K	$Sc_2(NH_2\text{-}BDC)_3$-293 K
formula unit	$Sc_2(C_8H_3NO_6)_3$	$Sc_2(C_8H_3NO_6)_3$	$Sc_2(C_8H_3NO_6)_3$	$Sc_2(C_8H_3NO_6)_3$	$Sc_2(C_8H_5NO_4)_3$	$Sc_2(C_8H_5NO_4)_3$
formula weight	717.26	717.26	717.26	717.26	627.31	627.31
calculated density/gcm^{-3}						
temperature/K	100	293	373	473	100	293
space group	*C*2/*c*	*C*2/*c*	*C*2/*c*	*C*2/*c*	*Fddd*	*Fddd*
X-ray source	synchrotron	synchrotron	synchrotron	synchrotron	synchrotron	Cu K_α
diffractometer	beamline I11	beamline I11	beamline I11	beamline I11	beamline I11	STOE STADI P
wavelength (Å)	0.826019	0.825028	0.825028	0.825028	0.826019	1.54056
unit cell (Å)						
a/Å	8.6674(2)	8.66399(7)	8.6614(7)	8.65457(8)	8.72068(16)	8.6995(4)
b/Å	34.3485(3)	34.42204(13)	34.42917(12)	34.43651(13)	20.82072(17)	20.8176(8)
c/Å	11.42264(15)	11.42526(6)	11.42032(6)	11.41078(6)	34.3857(3)	34.3571(12)
β/deg	115.2333(12)	114.9321(5)	114.8277(4)	114.6647(5)	90	90
volume/Å^3	3076.19(8)	3089.83(3)	3090.83(3)	3090.52(3)	6243.44(13)	6222.2(4)
no. reflections	625	406	407	407	518	701
no. atoms (non-H)	29	29	29	29	13	13
no. restraints	85	67	71	70	39	29
R	0.0552	0.0484	0.0469	0.0471	0.05	0.046
wR	0.072	0.0667	0.0647	0.0672	0.0681	0.0606
max. and min residual e- density (e/Å^3)	0.436, −0.453	0.293, −0.441	0.353, −0.435	0.336, −0.420	0.718, −0.761	0.854, −0.61

Sc species in the functionalized Sc_2BDC_3. Additionally, the peaks in the spectra for the $Sc_2(NH_2\text{-}BDC)_3$ and $Sc_2(NO_2\text{-}BDC)_3$ are shifted downfield relative to the unfunctionalized material, consistent with a smaller quadrupolar interaction.

Room temperature ^{13}C (14.1 T) CP MAS NMR spectra for Sc_2BDC_3 and the functionalized analogues are shown in Figure 5. For the two functionalized frameworks, ^{13}C CP MAS NMR spectra were recorded with a range of cross-polarization contact times between 0.25−3 ms (as shown in Figure 5b) to distinguish aromatic CH and quaternary carbons. The spectrum for Sc_2BDC_3 (reproduced from ref 11) has been assigned previously using density functional theory (DFT) calculations. Resonances are observed in two main groups, with aromatic carbons between 120 and 140 ppm and carboxylate carbons between 170 and 180 ppm. Within the aromatic region, protonated carbons are observed at lower chemical shift, while quaternary carbons are found at higher chemical shift. Considering the carboxylate region of the spectrum (and ignoring the small amount of impurity signal) the 2:1 doublet-like appearance of the resonance (see inset) is consistent with the two different terephthalate linkers (and their populations) in the structure.[10,25]

Addition of the functional groups lowers the symmetry of the terephthalate linker, resulting in more complex ^{13}C CP MAS NMR spectra for $Sc_2(NH_2\text{-}BDC)_3$ and $Sc_2(NO_2\text{-}BDC)_3$. In the spectrum for $Sc_2(NH_2\text{-}BDC)_3$, shown in Figure 5a, the resonance corresponding to the C1 site is shifted downfield owing to the electron withdrawing effect of the directly bonded nitrogen. In the variable-contact time ^{13}C CP MAS NMR spectra, shown in Figure 5b, the quaternary carbons C1, C3, and C6 exhibit much slower CP build-up rates than the CH carbons C2, C4 and C5 owing to the absence of directly bonded protons. The assignment of the aromatic carbon sites is supported by DFT calculations performed on an isolated 1-aminoterephthalate molecule (see Supporting Information for further details).

In the ^{13}C CP MAS NMR spectrum of $Sc_2(NO_2\text{-}BDC)_3$, shown in Figure 5, the C1 carbon is again shifted downfield owing to the electron withdrawing effect of the directly bonded NO_2 group. Aromatic CH and quaternary carbons are distinguished in variable-contact time ^{13}C CP MAS NMR spectra, shown in Figure 5b. The quaternary C3 resonance at 137.1 ppm exhibits a relatively slow CP build-up rate, while the unresolved resonances corresponding to CH carbons C4 and C5 at 132.6 ppm show almost constant intensity over the range of contact times used. The overlap of the quaternary C6 and CH C2 carbons at 125.3 ppm results in a more complex build-up profile. This assignment is again supported by DFT calculations on an isolated 1-nitroterephthalate molecule (see Supporting Information for further details).

3.2. Structure and Thermal Behavior of Sc_2BDC_3. Room temperature diffraction analysis of synchrotron X-ray data (293 K) shows the Sc_2BDC_3 structure to be orthorhombic *Fddd* (a = 8.74585(1) Å, b = 20.74387(2) Å, c = 34.34896(4) Å). Upon cooling under vacuum, the structure was observed to stay in the orthorhombic system down to 200 K below which a reversible symmetry change to monoclinic *C*2/*c* was observed (a = 8.7543(1) Å, b = 34.3853(1) Å, c = 11.14542(8) Å, β = 111.4791(8)°). In previous laboratory single crystal experiments performed in a stream of cool N_2 measured to be at 100 K, an orthorhombic structure was reported.[25] The discrepancy may derive from the presence of disordered air molecules adsorbed in the pores at that temperature when the single-crystal was cooled down and/or to the crystal temperature being greater than 100 K: there is no doubt from the synchrotron powder X-ray data that the structure at 200 K and below is monoclinic.

Whereas there are two unique terephthalate species in the asymmetric unit of the orthorhombic structure there are three in the monoclinic structure (Figure 6). In addition there are two types of unidirectional channels in the monoclinic model as

opposed to one in the orthorhombic structure. The symmetry change arises from a translation of alternate scandium carboxylate chains leading to deviation from 90° of the angle between the axis of the linker 1 terephthalate and the scandium carboxylate chain. This translation results in an associated rotation in the ScO_6 octahedra which causes the previously symmetry-related linker 2 terephthalates to rotate in opposite directions leading to two nonequivalent positions and therefore two different channels.

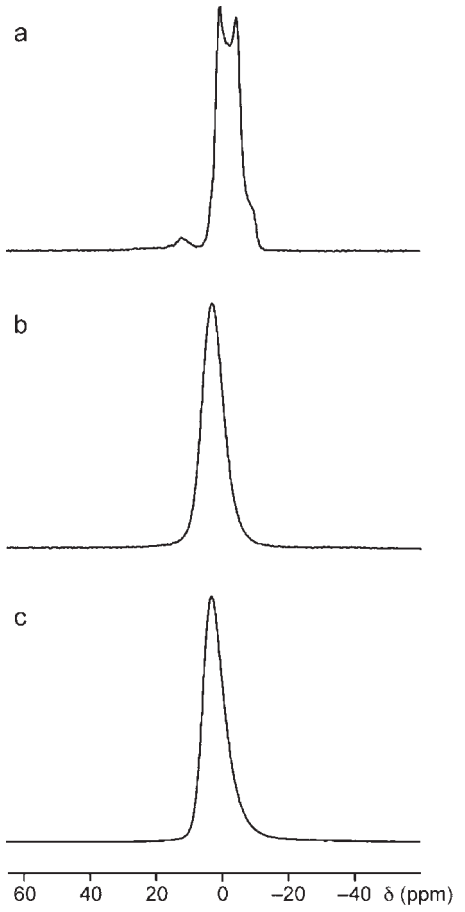

Figure 4. ^{45}Sc (9.4 T) MAS NMR spectra of (a) Sc_2BDC_3, (b) $Sc_2(NH_2\text{-}BDC)_3$, and (c) $Sc_2(NO_2\text{-}BDC)_3$ recorded at a MAS rate of 12.5 kHz and at room temperature. Panel (a) adapted with permission from ref 11. Copyright 2011 Elsevier.

Plotting the unit cell volume of the orthorhombic phase as a function of temperature shows a significant negative thermal expansion (NTE) of the structure from 250−623 K, with a linear expansivity of 2.4×10^{-5} K^{-1} (Figure 7). This behavior is consistent with the work of Keppert et al. on the zinc terephthalate MOF-5, which has an isotropic linear (volume) thermal expansivity of 4.0×10^{-5} K^{-1} over a similar temperature range. Careful structural analysis of single crystal diffraction on MOF-5 indicated the NTE behavior results from the twisting and vibrating of the carboxylate group and the out-of-phase translation and vibration of the aromatic ring.[6] For the orthorhombic Sc_2BDC_3, the NTE is linear over the region studied, but in this case the expansion upon cooling is highly anisotropic. The change in the cell parameters shows a small expansion of the z axis and contraction of the y axis (Figure 8) but the most significant change observed was the shortening of the x axis. This shortening is along the scandium carboxylate chain and is consistent with twisting and vibrating of the carboxylate group and as a consequence a shortening of the Sc--Sc distance along the chains as illustrated in Figure 8.

The cell volume over the low temperature range 140−225 K remains almost constant. It is possible that the symmetry change from orthorhombic to monoclinic results in a reduction in cell volume that counteracts the cell volume expansion predicted from the trend observed in the orthorhombic region. In the case of MOF-5, a linear trend of expansion is observed from 500 K down to 100 K, so the same effect of reduced translation and libration upon cooling might also be expected in this case.

3.3. Variable-Temperature ^2H Solid-State NMR. ^2H solid-state NMR offers a convenient method for probing motional processes that take place on the microsecond time scale. This approach has been used to observe and determine the rate

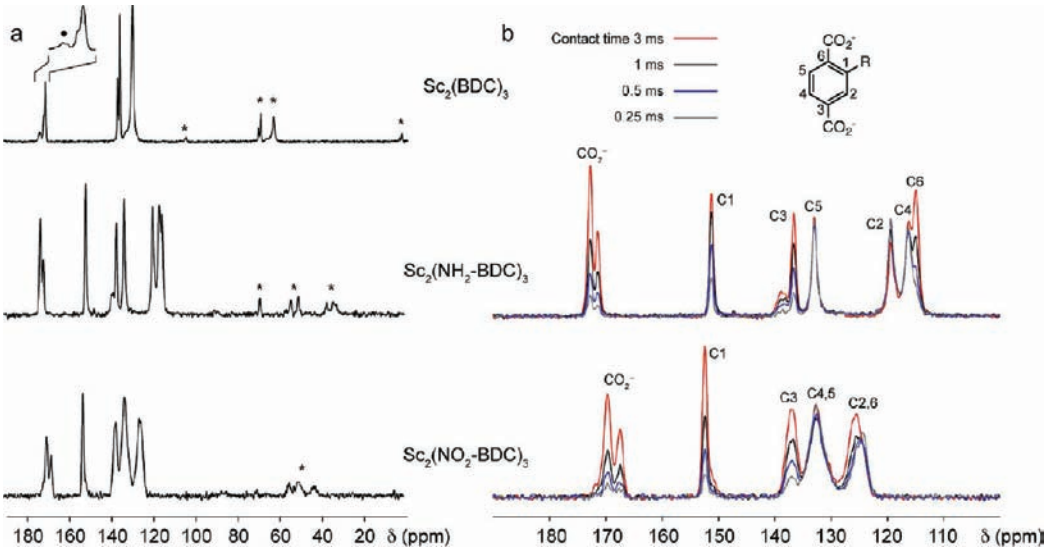

Figure 5. (a) ^{13}C (14.1 T) CP MAS NMR spectra of unfunctionalized and functionalized Sc_2BDC_3 MOFs recorded at a MAS rates of between 10 and 12.5 kHz and at room temperature. (b) Expanded carboxylate and aromatic regions of variable-contact time ^{13}C CP MAS NMR of functionalized Sc_2BDC_3 MOFs. Spinning sidebands are indicated by an asterisk *. A low-intensity resonance corresponding to a small impurity in (a) is denoted by a black dot •. Panel (a) adapted with permission from ref 11. Copyright 2011 Elsevier.

dx.doi.org/10.1021/ic201387d |Inorg. Chem. 2011, 50, 10844–10858

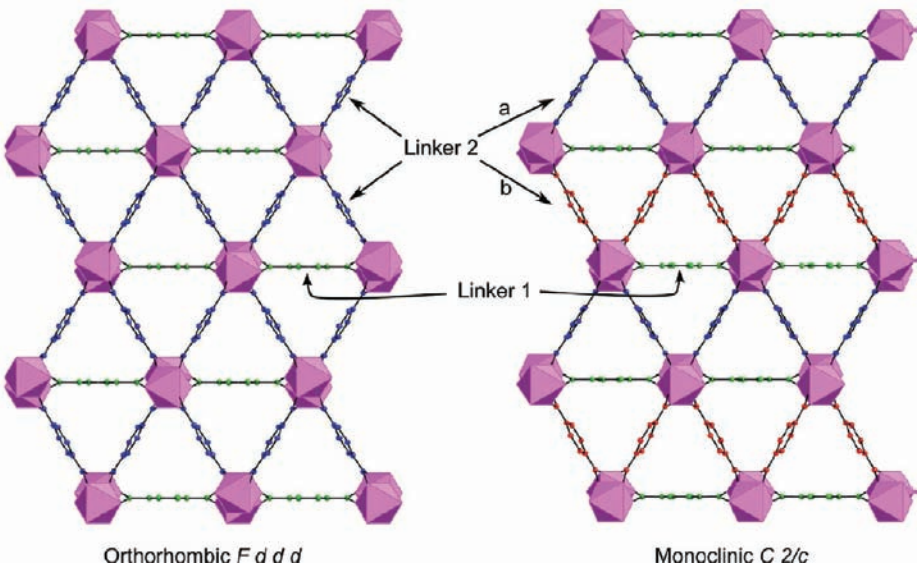

Figure 6. Comparison of the orthorhombic (*Fddd*) and monoclinic (*C2/c*) models for Sc_2BDC_3 with the number of symmetry related terephthalates identified by the color. (Models taken from literature single-crystal diffraction experiments on Sc_2BDC_3 at the ESRF.[10]).

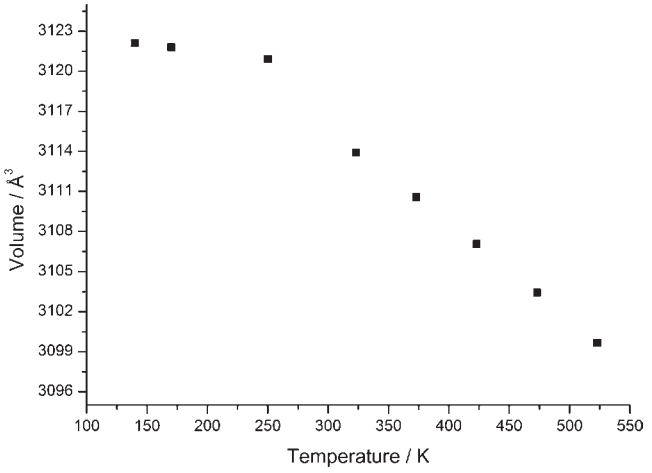

Figure 7. Unit cell volume of monoclinic and half unit cell volume of orthorhombic Sc_2BDC_3 against temperature. Error bars within the points.

of ring flipping reorientations of benzene rings in MIL-47(V) and MIL-53(Cr),[26] and to characterize the dynamics of phenylene rotors in mesoporous *p*-phenylenesilica.[27] To determine if similar processes occur in Sc_2BDC_3, ^{2}H NMR experiments were performed on a static sample which was synthesized using fully deuterated benzene dicarboxylic acid. ^{2}H wide-line NMR spectra recorded in the temperature range 298−383 K are shown in Figure 9a. At room temperature, the spectrum is dominated by a characteristic Pake doublet powder line shape, with a pair of singularities, or "horns", separated by ∼130 kHz. However, a second pair of low-intensity horns, separated by approximately 30 kHz, is also observed near the center of the spectrum. With increasing temperature, pronounced changes in the line shape are observed as the central pair of horns increase in intensity relative to the outer horns. To interpret these results, simulations were performed using the EXPRESS software package.[28] ^{2}H wide-line NMR spectra were simulated assuming a 180° flip around the C_2 axis of a deuterated benzene ring with deuterium C_Q's of 210 kHz and η_Q of 0. Simulations were performed for a range of rate constants between 0 and 5×10^7 s^{-1}. The changes in the line shape in the simulated spectra, shown in Figure 9b, resemble those observed in the experimental spectra. However, at temperatures greater than 353 K, smaller changes in the experimental line shape are observed, and the spectra do not appear to exactly follow the changes in line shape predicted by the simulation. A possible explanation for the observed behavior is that one portion of the rings undergo ring flipping while another portion remains immobile or flips with a different rate constant. In this case, the observed spectrum would comprise a superposition of two powder patterns with different degrees of partial averaging, resulting in more complex changes in line shape with temperature. Indeed, given the presence of two crystallographically distinct linkers it is possible that they may each exhibit a different motional behavior. Attempts to characterize the two types of linker separately by ^{2}H MAS NMR were unsuccessful owing to the crystallographically distinct deuterium sites in the structure having the same chemical shift (see Supporting Information for further details).

3.4. Structure and Thermal Behavior of Functionalized Sc_2BDC_3. *$Sc_2(NH_2\text{-}BDC)_3$.* As described in the crystallography section, the NH_2-terephthalate structure was observed to possess orthorhombic symmetry at both 100 and 298 K. The structure is shown in Figure 10. For one of the terephthalate linkers, perpendicular to the scandium carboxylate chains (Linker 1 of Figure 6), -NH_2 groups are disordered over four symmetry related positions (shown in Figure 10b). The other, "linker 2" terephthalates lie at an angle (69.4°) to the scandium carboxylate chains (which run parallel to the *z* axis) and have two pairs of crystallographically distinct aromatic carbon atoms. In this case, only one set of pairs is found to possess amino groups as shown in Figure 10c, an amino group on the other pair of carbons would be too close to the adjacent carboxylate oxygen bound to the scandium (N---O = 2.70 Å). These amino groups are statistically disordered over the two equivalent positions on linker 2 terephthalates in the crystal: for consecutive rings

dx.doi.org/10.1021/ic201387d |*Inorg. Chem.* 2011, 50, 10844–10858

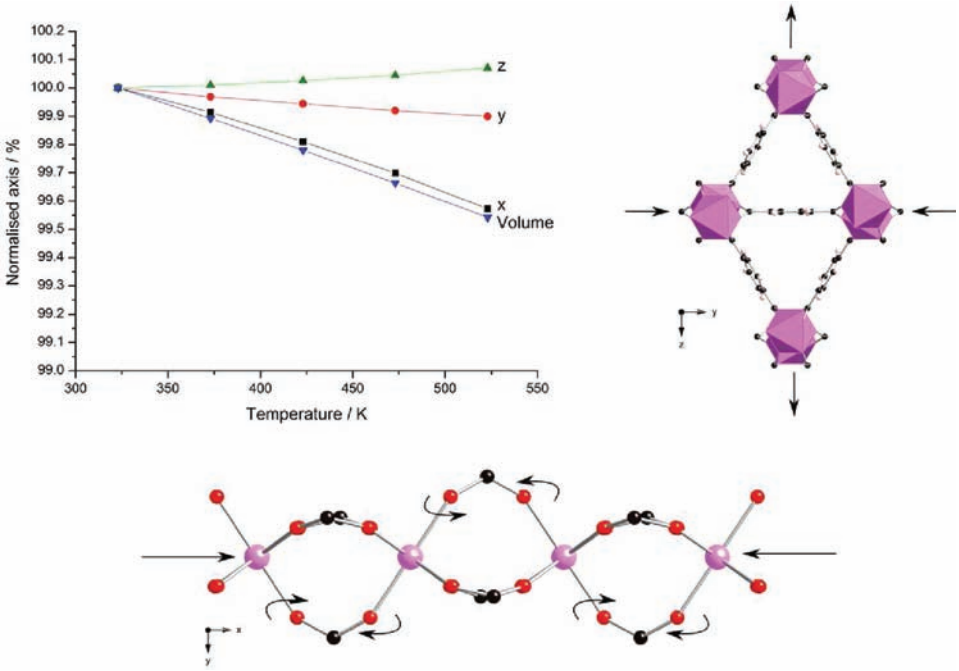

Figure 8. Variation of unit cell axis lengths and volume of orthorhombic Sc_2BDC_3, as a function of temperature between 323 and 523 K, expressed as percentages of their values at 323 K. Anisotropic volume change is observed as a consequence of small variations in the repeats along *y* and *z* and a significant shortening of the chain along *x* arising from twisting of the carboxylate units.

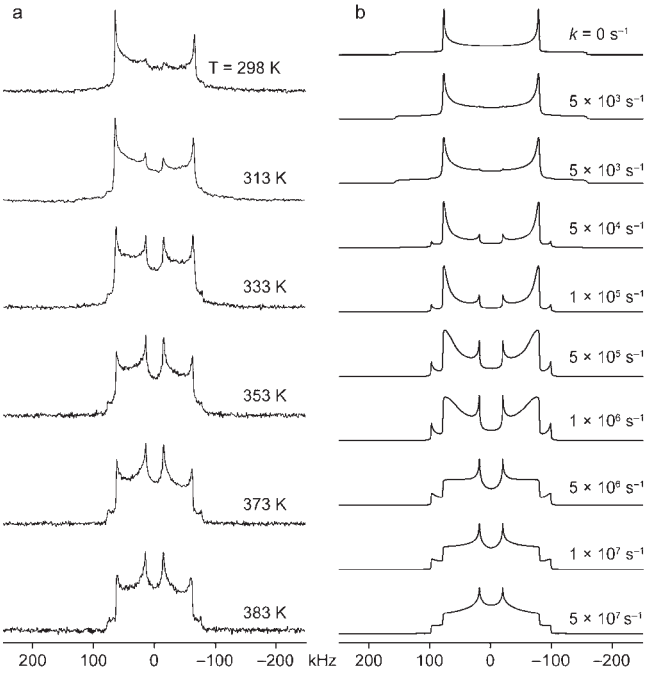

Figure 9. (a) Experimental ^2H (9.4 T) wide-line NMR spectra of fully deuterated Sc_2BDC_3 recorded at temperatures in the range 298−383 K. (b) ^2H wide-line NMR spectra simulated using the EXPRESS[28] simulation program assuming a 180° flip of a deuterated benzene ring with deuterium C_Q's of 210 kHz and η_Q of 0.

along the *x* axis the nearest N---N approach for a fully disordered distribution would be 3.1 Å. Assuming that the "unoccupied" position is sterically unfavorable, it would seem likely that 180° rotation of linker 2 terephthalates would be inhibited, because it would lead to motion from a favored to a disfavored orientation.

Room temperature powder diffraction data was also indexed in orthorhombic *Fddd* (Table 3). As there is no symmetry change to monoclinic on cooling to 100 K, as observed for the unfunctionalized material, this indicates that the amino group stabilizes the orthorhombic structure. We suggest that this is due to favorable interactions between H-atoms of the amino-group and the O-atoms of the carboxylate-group in the orthorhombic structure. N···O distances of 3.44 Å and 3.58 Å are observed (shown in the Supporting Information). It does not appear to be a steric effect of the $-NH_2$ group, because Sc_2BDC_3 functionalized with the much larger $-NO_2$ group adopts the monoclinic structure.

$Sc_2(NO_2$-BDC)$_3$. The nitro-functionalized Sc_2BDC_3 structure was indexed as monoclinic at room temperature (293 K) and on cooling to low temperature (100 K) stayed monoclinic (Table 3). Attempts to produce the symmetry change by further heating to 473 K were unsuccessful, suggesting that it would crystallize in the monoclinic space group (synthesis temperature 463 K). The structures obtained from powder diffraction and from single crystal diffraction (Figure 11) show a partial ordering of nitro groups on the "linker 2" terephthalates (designated 2a and 2b in the monoclinic structure) and also an ordering on the "linker 1" terephthalate. In each case the nitro group is rotated about 90° away from the plane of the ring. This occurs as a result of steric interactions with oxygen atoms of nearby carboxylate groups. Similar effects on $-NO_2$ group orientation with respect to aromatic rings have been observed from compilations of structural data from molecular crystal structures of molecules with benzene rings that possess $-NO_2$ groups with two neighboring aromatic substituents.[29,30]

The ordering of $-NO_2$ groups and the monoclinic symmetry at room temperature arises because the bulky nitro group prevents the terephthalate unit from being arranged perpendicularly to the

dx.doi.org/10.1021/ic201387d |*Inorg. Chem.* 2011, 50, 10844–10858

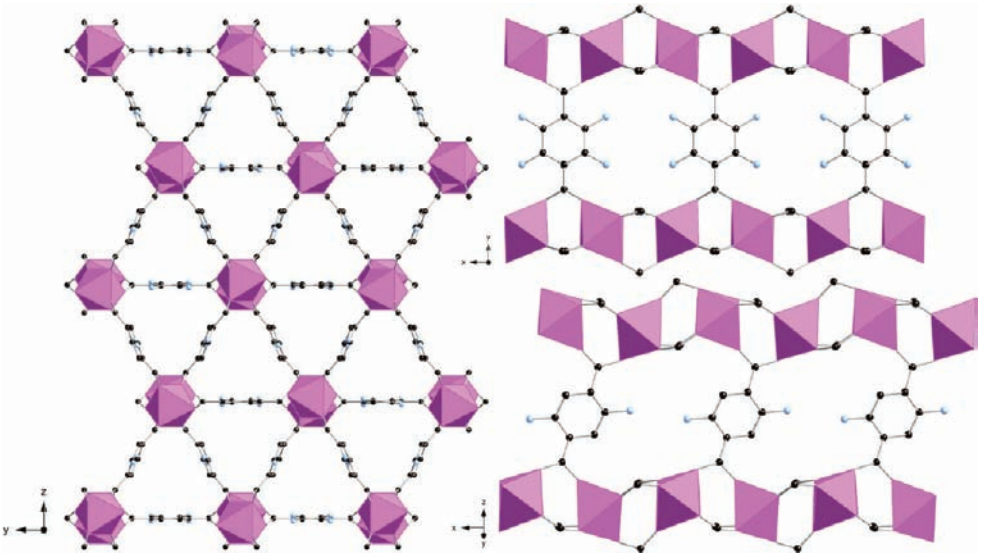

Figure 10. $Sc_2(NH_2\text{-}BDC)_3$ (100 K) viewed down the channel (x) axis (left) and the columns of "linker 1" (right top) and "linker 2" (right bottom) terephthalate linkers. In each case all symmetry related positions of $-NH_2$ groups are shown: only one-quarter or one-half of these sites are occupied.

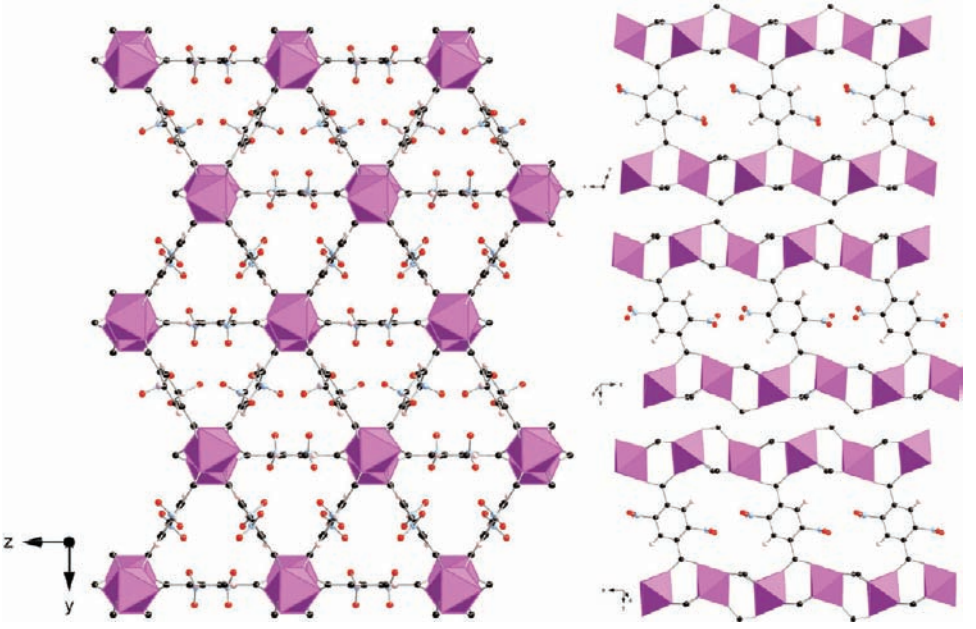

Figure 11. Structure of $Sc_2(NO_2\text{-}BDC)_3$ (as determined by single crystal diffraction) viewed down the channel (x) axis (left) and columns of "linker 1" (right top), "linker 2a" (right middle), and "linker 2b" (right bottom) terephthalates. In each case all symmetry related positions of $\text{-}NO_2$ groups are shown: only one-half of these sites are occupied, and the closeness of their approach indicates all groups along one row of terephthalate units will be oriented in the same direction. Note that this partial ordering precludes rotation of the terephthalate units.

chains of isolated ScO_6 octahedra, again because of steric considerations. Distance and angles were taken from the single crystal structural data. The angle of 96.12° that the terephthalate makes to the chain means that the nitro group oxygen atoms are 3.12 Å from the nearest carboxylate oxygens, compared with 2.8 Å if the terephthalate were perpendicular to the chains, as it would be in the orthorhombic symmetry. The bulky $\text{-}NO_2$ group therefore destabilizes $Sc_2(NO_2\text{-}BDC)_3$ in the orthorhombic form relative to the monoclinic form, so that the structure adopts monoclinic symmetry even at room temperature and above. The distances between observed locations of the sites for the nitro group along each row of terephthalates of types 1, 2a, or 2b adjacent along a (i.e., on the two crystallographically identical carbons on each ring) indicate it is likely that within each individual chain of terephthalates along a there is full ordering of the $\text{-}NO_2$ group but across the bulk structure it is disordered over the two sites.

The orientation of the $\text{-}NO_2$ groups with respect to the phenyl rings results in the projection of the oxygen atoms into the channels, which are already narrow. The estimated free diameters of openings at the narrowest points in the two channel systems are 1.95 and 2.40 Å, although there would be larger "cages"

dx.doi.org/10.1021/ic201387d |*Inorg. Chem.* 2011, 50, 10844–10858

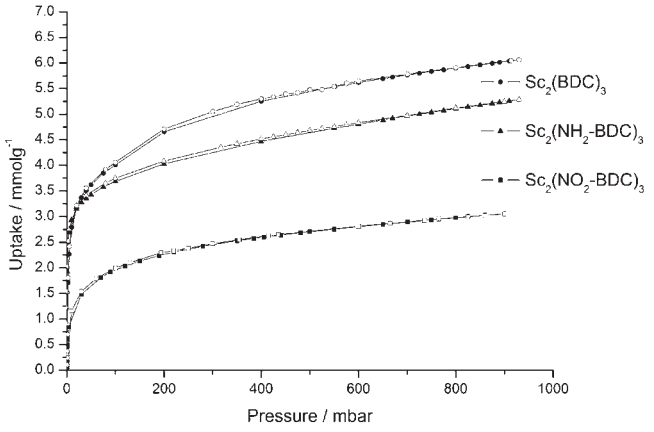

Figure 12. Carbon dioxide adsorption isotherms at 196 K on Sc_2BDC_3, $Sc_2(NH_2\text{-}BDC)_3$, and $Sc_2(NO_2\text{-}BDC)_3$. Filled symbols, adsorption branch; open symbols, desorption branch.

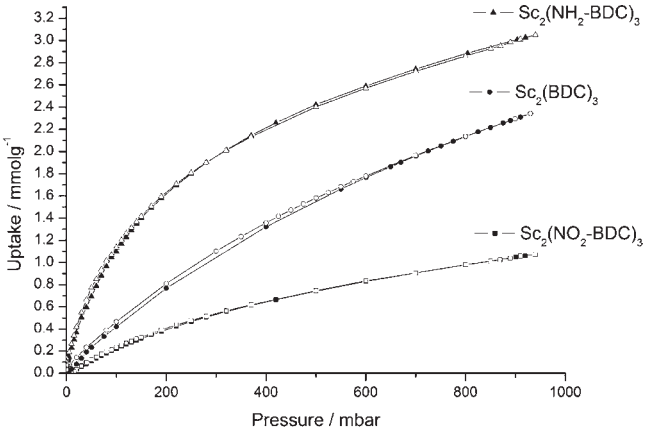

Figure 13. Carbon dioxide adsorption isotherms at 273 K on Sc_2BDC_3, $Sc_2(NH_2\text{-}BDC)_3$, and $Sc_2(NO_2\text{-}BDC)_3$. Filled symbols, adsorption branch; open symbols, desorption branch.

between these bottlenecks, the shape of which would depend on the location of $-NO_2$ groups disordered over symmetrically equivalent sites on the phenyl groups.

The deviation of the $-NO_2$ form at 100 K from orthorhombic (i.e., the monoclinicity), measured by a change in the tilt of the linker 1 terephthalate from 90° in the orthorhombic structure, is much larger in the $-NO_2$ structure (83.9°) than in the unfunctionalized monoclinic Sc_2BDC_3 (86.2°), indicating a significant steric effect of the $-NO_2$. This results in a reduction of the unit cell volume from 3122 to 3076 Å^3, a decrease of 1.5%, despite the inclusion of a bulky $-NO_2$ group.

In summary, powder X-ray diffraction of the parent Sc_2BDC_3 indicates that at between 200 and 225 K the structure distorts from orthorhombic to monoclinic, the mechanism of which is a concerted rotation of carboxylate groups. This phase transition is prevented in $Sc_2(NH_2\text{-}BDC)_3$ by the presence of interactions between the $-NH_2$ group and adjacent carboxylate O atoms, but in $Sc_2(NO_2\text{-}BDC)_3$ the presence of bulky nitro groups stops the framework adopting the orthorhombic structure even at 473 K, and strong partial ordering of nitro groups is observed over all terephthalate linkers. Comparison of different monoclinic variants show the scandium terephthalate framework is itself quite flexible, and varies with temperature and the nature of substituents.

3.5. Adsorption. Adsorption of N_2 at 77 K gives a pore volume of 0.26 cm^3 g^{-1} at $P/P_0 = 0.1$ for Sc_2BDC_3. The inclusion of $-NH_2$ groups reduces porosity to 0.148 cm^3 g^{-1} (reduced by 43%) and inclusion of $-NO_2$ groups renders the material nonporous to N_2. This suggests the amino groups do not project strongly into the channels (although they do take up space in gaps in the channel walls) whereas the O atoms of the nitro groups are known to project significantly into the channels, reducing the size of the constrictions below the diameter of N_2 molecules (2-center L-J diameter 3.26 Å). In addition, at 77 K these groups are not likely to undergo rapid reorientational motion to permit diffusion of gas molecules.

3.5.1. CO_2 Adsorption. Adsorption isotherm data at 196 and 273 K up to 1 bar of CO_2 on Sc_2BDC_3 and its functionalized variants are reported in Figures 12 and 13. Adsorption isotherms of CO_2 on Sc_2BDC_3 have been reported previously, and the single crystal structure at 235 K and 1 bar CO_2 was determined as monoclinic, with a maximum uptake of CO_2 in this structure of 3.5 mmol g^{-1}.[10] Since the empty structure at 235 K is expected from the current work to be orthorhombic, it appears that the adsorption of CO_2 stabilizes the monoclinic structure via sorbate-sorbent interactions.

To investigate this further, GCMC simulations were performed using the monoclinic and orthorhombic models for the scandium terephthalate framework assuming a temperature of 235 K, for which crystallographic data is available. Two monoclinic structures were taken, one refined against the X-ray powder diffraction data at 170 K from this study (mono-170) and the other from the single crystal structure X-ray diffraction experiments of CO_2 adsorbed on Sc_2BDC_3 at 235 K and 1 bar (mono-CO_2). The orthorhombic structure was that measured previously at 298 K. Full results of the simulations performed on Sc_2BDC_3 with and without functional groups will be reported later, but Figure 14 shows the simulated locations of 3.5 mmol g^{-1} of CO_2 in the three different simulated structures, compared with the structure measured experimentally at this uptake (at 235 K, 1 bar).

All channels in the orthorhombic structure are identical, whereas there are two types in the monoclinic structures. In each of the orthorhombic and mono-170 structures, there is considerable disorder in the orientation of the CO_2 molecules, but in the mono-CO_2 structure the molecules show a much higher degree of order in both sets of channels, which is consistent with the structure observed experimentally at 235 K. The ordering would be expected to stabilize the guest−host assembly enthalpically. This indicates that the structure of Sc_2BDC_3 adapts to "fit" the CO_2 adsorbate. This is manifested, for example, by a change in the tilt of terephthalate linkers 2a and b with respect to the channel axis, and by a change in the monoclinic angle. Previous work shows that adsorption at 230 K of larger molecules, such as methane and ethane, is achieved in Sc_2BDC_3 that remains orthorhombic. This indicates that Sc_2BDC_3 is a flexible structure, which can distort from orthorhombic to monoclinic above the phase transition temperature in response to sorption of molecules of appropriate size, and that the degree of that distortion is variable, according to the size and shape of the adsorbate molecules.

The adsorption data at 196 K (Figure 12) shows a slight step at an uptake of about 4 mmol g^{-1}, which was observed previously (see expanded version, Supporting Information). This type of step in the isotherm might be explained either by a change in the arrangement of CO_2 molecules in the monoclinic form, or as

dx.doi.org/10.1021/ic201387d |*Inorg. Chem.* 2011, 50, 10844–10858

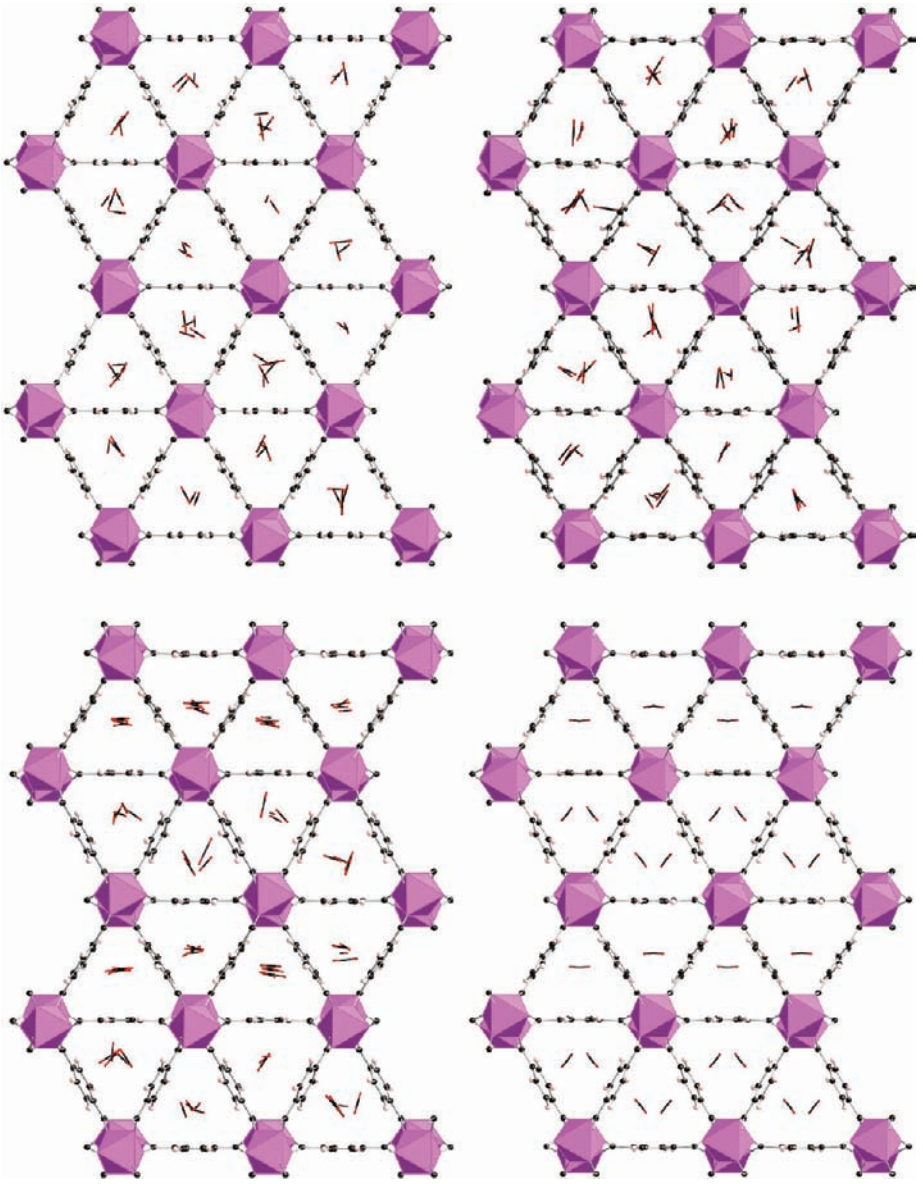

Figure 14. Snapshots of simulated CO_2 adsorption at 235 K and a loading of 3.5 mmol g^{-1} inside Sc_2BDC_3 orthorhombic model (top left), Sc_2BDC_3 monoclinic model (top right) from temperature series at 170 K, Sc_2BDC_3_CO_2 single crystal structure (bottom left) compared to the positions identified by single crystal (bottom right). CO_2 positions are indicated by the red/black stick representation in the framework model.

seems more likely from this preliminary modeling, a change in the symmetry to orthorhombic, with larger cell volume, that could accommodate more molecules. A similar effect has been observed for ZIF-8 in the uptake of N_2, where the imidazolate groups rotate to give a new structure that allows greater uptake.[31] Modeling and experimental studies are ongoing to resolve the cause of this observed effect.

Low temperature adsorption data (196 K) for CO_2 shows that the addition of -NH_2 and -NO_2 groups to the Sc_2BDC_3 results in a decrease in the maximum adsorption capacity of the material (which for the unfunctionalized solid is 6 mmol g^{-1}). The decrease in capacity is relatively small (−13%) for the amino-functionalized form, especially when the increased mass of the functionalized solid (+8%) is taken into account. That the CO_2 capacity (196 K) is reduced less by amino-functionalization than the N_2 capacity (77 K) could be due to differences in stacking of the two types of differently sized molecules. It may be that the longer CO_2 molecules stack predominantly along the channels and are less affected by the presence of the functional groups between the rings. In addition, some pore blocking by -NH_2 groups could reduce the uptake of the larger N_2 molecules in the functionalized solid.

Analysis of the low pressure region shows that there is a higher uptake at low *P* (<30 mbar at 196 K) for the amino-terephthalate form. The reduction in CO_2 adsorption capacity of the NO_2-functionalized solid (−50%) is much greater than the change in mass (+24%). The decrease arises from the occupation of space in the channels by the nitro group O atoms. That 3 mmol g^{-1} can still be taken up is remarkable, given the narrow bottlenecks in the triangular channels measured crystallographically. These openings are smaller than the L-J diameter (across the molecule) of CO_2, 2.98 Å, so that the ability of $Sc_2(NO_2\text{-}BDC)_3$ to take up

dx.doi.org/10.1021/ic201387d |*Inorg. Chem.* 2011, 50, 10844–10858

CO_2 must be attributed to the ability of -NO_2 groups to rotate to allow CO_2 molecules to pass. The lack of a gate-opening effect (which would give a step in the isotherm and hysteresis) suggests that the activation energy required for window opening is available from thermal energy and interaction energy between the CO_2 and the $Sc_2(NO_2\text{-BDC})_3$ even at the lowest partial pressures.

Adsorption of CO_2 at 273 K up to 900 mbar (Figure 13) is able to distinguish between the solids on the basis of their strengths of adsorption. Notably, samples of each solid loaded at 293 K with 1 bar of CO_2 showed that under these similar conditions they did not change symmetry from the empty structures. While the uptake of $Sc_2(NO_2\text{-BDC})_3$ is lower than that of Sc_2BDC_3 as expected from the available porosity measured at 196 K, the $Sc_2(NH_2\text{-BDC})_3$ shows an increased uptake which is particularly marked at lower pressures. This derives from a higher heat of interaction of CO_2 with the amine groups. Similar effects have been predicted theoretically.[32] Combining these effects of functionalization may be of use in tuning the adsorption and selectivity of the material for specific applications in gas storage and separation.

4. CONCLUSIONS

The 2-amino- and 2-nitroterephthalate forms of the scandium terephthalate MOF, Sc_2BDC_3 have been synthesized for the first time by means of hydrothermal synthesis, using Sc_2O_3 (or $Sc(NO_3)_3$ for $Sc_2(NO_2\text{-BDC})_3$) as the scandium source. The crystal structure of these and the unmodified Sc_2BDC_3 have been measured by Rietveld refinement against X-ray powder diffraction data at 100 K. Whereas Sc_2BDC_3 and the -NO_2 forms adopt monoclinic *C*2/*c* symmetry at this temperature, the amino form has orthorhombic *Fddd* symmetry. Strong partial ordering effects are observed in the location of functional groups: in the orthorhombic -NH_2 form the groups are ordered over one of two sites on one linker, and disordered over C atoms on the second linker, whereas in the monoclinic -NO_2 form the groups are ordered over one in two possible carbons on each of the crystallographically distinct terephthalate groups. Statistical disorder over symmetrically equivalent C atoms remains, although within rows of at least some of the terephthalate linkers it is likely for steric reasons that the functional groups will take up the same orientation in adjacent linkers.

As the temperature of Sc_2BDC_3 is raised, it undergoes a phase transition to orthorhombic at 225 K, characterized by synchrotron X-ray diffraction on a powder sample. The orthorhombic form demonstrates negative thermal expansivity over the range 225−523 K, which can be attributed to libration and translation of the aromatic rings. In addition, at least one of two crystallographically distinct phenyl groups shows π flips as shown by ^2H wide-line NMR spectroscopy over the measured temperature range 333−383 K. Upon raising the temperature from 100 to 293 K, the -NH_2 form remains orthorhombic and the NO_2-form remains monoclinic even if the temperature is raised to 473 K. That the -NH_2 form remains orthorhombic is attributed to stabilization via interaction of the amine group H atom with a carboxylate oxygen, whereas the steric effect of the -NO_2 group acts to prevent the monoclinic structure becoming orthorhombic at room temperature or above. The structural changes that are observed in this series of compounds therefore demonstrate the flexibility possible even in MOFs that do not exhibit the extreme breathing effects shown by MIL-53 or MIL-88. This flexibility arises from the rotation of carboxylate groups with respect to the aromatic rings of the terephthalate linkers and the hinge-like motion of the carboxylate groups where they are coordinated to the metal cations.

The CO_2 adsorption behavior of Sc_2BDC_3, reported previously, can be interpreted in terms of favored uptake of CO_2 by the monoclinic rather than the orthorhombic form, at least for uptakes less than about 4 mmol g^{-1}. Molecular modeling indicates ordering in the monoclinic form (as observed experimentally) whereas CO_2 would not occupy such well-defined sites in the orthorhombic structure. The CO_2 adsorption on Sc_2BDC_3 is strongly affected by functionalization. Amino groups reduce the adsorption capacity but increase the uptake at low pressures, because of stronger interactions with the CO_2. Remarkably, while -NO_2 groups reduce CO_2 uptake, as expected from their steric bulk and the reduction in cell volume that results from the change in symmetry to monoclinic that their inclusion induces, they do not block off the porosity as might be expected from the crystal structure. It is likely that the -NO_2 groups can rotate and the framework structure adjusts to enable CO_2 molecules to diffuse through the channels and gain access to the cage-like porosity located between the O atoms of the -NO_2 groups that project into the channels.

Although at first glance a relatively simple and rigid structure, close examination of Sc_2BDC_3 and its functionalized analogues reveals a wealth of structural adaptation is possible, with flexibility and reorientation mechanisms that operate over a range of different temperatures and time scales and which have important consequences for determining its adsorption behavior.

■ ASSOCIATED CONTENT

Supporting Information. Simulation details, NMR methods and assignments, powder diffraction data, TGA analyses and crystallographic data (CIFs). This material is available free of charge via the Internet at http://pubs.acs.org.

■ AUTHOR INFORMATION

Corresponding Author
*E-mail: paw2@st-andrews.ac.uk.

■ ACKNOWLEDGMENT

Funding for this work was provided by the European Commission FP6 (S.R.M., P.A.W., 'DESANNS' (SES6-CT-2005-020133), the EPSRC (V.R.S, J.M.G., and S.E.A., EP/E041825/1; D.F.-J. thanks the European Commission for a Marie Curie Intra-European fellowship (PIEF-GA-2009-236665); A.-M.B., T.D., EP/F009208/1 and the University of St Andrews. The authors thank Professor Chiu C. Tang for assistance at the I11 beamline at the Diamond Light Source (DLS) and DLS for beamtime and Professor Alexandra M. Z. Slawin (University of St Andrews) for single-crystal data collection and helpful discussion.

■ REFERENCES

(1) Loiseau, T.; Serre, C.; Huguenard, C.; Fink, G.; Taulelle, F.; Henry, M.; Bataille, T.; Férey, G. *Chem.—Eur. J.* **2004**, *10*, 1373.
(2) Surblé, S.; Serre, C.; Mellot-Draznieks, C.; Millange, F.; Férey, G. *Chem. Commun.* **2006**, 284.
(3) Serre, C.; Mellot-Draznieks, C.; Surblé, S.; Audebrand, N.; Filinchuk, Y.; Férey, G. *Science* **2007**, *315*, 1828.

(4) Li, H.; Eddaoudi, M.; O'Keeffe, M.; Yaghi, O. M. *Nature* **1999**, *402*, 276.
(5) Gonzalez, J.; Devi, R. N.; Tunstall, D. P.; Cox, P. A.; Wright, P. A. *Microporous Mesoporous Mater.* **2005**, *84*, 97.
(6) Lock, N.; Wu, Y.; Christensen, M.; Cameron, L. J.; Peterson, V. K.; Bridgeman, A. J.; Kepert, C. J.; Iversen, B. B. *J. Phys. Chem. C* **2010**, *114*, 16181.
(7) Gould, S. L.; Tranchemontagne, D.; Yaghi, O. M.; Garcia-Garibay, M. A. *J. Am. Chem. Soc.* **2008**, *130*, 3246.
(8) Kolokolov, D. I.; Jobic, H.; Stepanov, A. G.; Guillerm, V.; Devic, T.; Serre, C.; Férey, G. *Angew. Chem., Int. Ed.* **2010**, *49*, 4791.
(9) Devic, T.; Horcajada, P.; Serre, C.; Salles, F.; Maurin, G.; Moulin, B.; Heurtaux, D.; Clet, G.; Vimont, A.; Greneche, J. M.; Le Ouay, B.; Moreau, F.; Magnier, E.; Filinchuk, Y.; Marrot, J.; Lavalley, J. C.; Daturi, M.; Férey, G. *J. Am. Chem. Soc.* **2010**, *132*, 1127.
(10) Miller, S. R.; Wright, P. A.; Devic, T.; Serre, C.; Férey, G.; Llewellyn, P. L.; Denoyel, R.; Gaberova, L.; Filinchuk, Y. *Langmuir* **2009**, *25*, 3618.
(11) Mowat, J. P. S.; Miller, S. R.; Slawin, A. M. Z.; Seymour, V. R.; Ashbrook, S. E.; Wright, P. A. *Microporous Mesoporous Mater.* **2011**, *142*, 322.
(12) Thompson, S. P.; Parker, J. E.; Potter, J.; Hill, T. P.; Birt, A.; Cobb, T. M.; Yuan, F.; Tang, C. C. *Rev. Sci. Instrum.* **2009**, 80.
(13) Antonijevic, S.; Wimperis, S. *J. Magn. Reson.* **2003**, *164*, 343.
(14) Larson, A. C.; Von Dreele, R. B. General Structure Analysis System. Los Alamos National Laboratory Report LAUR 86-748; Los Alamos National Laboratory: Los Alamos, NM, 1994.
(15) Toby, B. H. *J. Appl. Crystallogr.* **2001**, *34*, 210.
(16) Le Bail, A. *Powder Diffr.* **2005**, *20*, 316.
(17) Boultif, A.; Louer, D. *J. Appl. Crystallogr.* **2004**, *37*, 724.
(18) Crystal data for $Sc_2(NO_2\text{-}BDC)_3$: $Sc_2C_{24}H_9N_3O_{18}$, $M_r = 717.26$, monoclinic $C2/c$, $a = 8.669(4)$ Å, $b = 34.370(15)$ Å, $c = 11.053(6)$ Å, $\beta = 110.486(6)°$, $V = 3085.01$ Å^3, $D_c = 1.544$ g/cm^3, RI = 0.157.
(19) Frenkel, D.; Smit, B. *Understanding Molecular Simulation: From Algorithms to Applications*, 2nd ed.; Academic Press: San Diego, CA, 2002.
(20) Gupta, A.; Chempath, S.; Sanborn, M. J.; Clark, L. A.; Snurr, R. Q. *Mol. Simul.* **2003**, *29*, 29.
(21) (a) Peng, D.-Y.; Robinson, D. B. *Ind. Eng. Chem., Fundam.* 1976, 15, 59−64. Reid, R. C.; Pausnitz, J. M.; Poling, B. E. *The Properties of Gases and Liquids*, 4th ed.; McGraw-Hill Companies: New York, 1987.
(22) Mayo, S. L.; Olafson, B. D.; Goddard, W. A. *J. Phys. Chem.* **1990**, *94*, 8897.
(23) Potoff, J. J.; Siepmann, J. I. *AIChE J.* **2001**, *47*, 1676.
(24) Clark, S. J.; Segall, M. D.; Pickard, C. J.; Hasnip, P. J.; Probert, M. J.; Refson, K.; Payne, M. C. *Z. Kristallogr.* **2005**, *220* (5−6), 567–570.
(25) Miller, S. R.; Wright, P. A.; Serre, C.; Loiseau, T.; Marrot, J.; Férey, G. *Chem. Commun.* **2005**, 3850.
(26) Kolokolov, D. I.; Jobic, H.; Stepanov, A. G.; Plazanet, M.; Zbiri, M.; Ollivier, J.; Guillerm, V.; Devic, T.; Serre, C.; Férey, G. *Eur. Phys. J.: Special Topics* **2010**, *189*, 263.
(27) Comotti, A.; Bracco, S.; Valsesia, P.; Beretta, M.; Sozzani, P. *Angew. Chem., Int. Ed.* **2010**, *49*, 1760.
(28) Vold, R. L.; Hoatson, G. L. *J. Magn. Reson.* **2009**, *198*, 57.
(29) Grabowski, S. J.; Krygowski, T. M. *Acta Crystallogr., Sect. C* **1985**, *41*, 1224.
(30) Deridder, D. J. A.; Schenk, H. *Acta Crystallogr., Sect. B* **1995**, *51*, 221.
(31) Fairen-Jimenez, D.; Moggach, S. A.; Wharmby, M. T.; Wright, P. A.; Parsons, S.; Düren, T. *J. Am. Chem. Soc.* **2011**, *133*, 8900–8902.
(32) Torrisi, A.; Bell, R. G.; Mellot-Draznieks, C. *Cryst. Growth Des.* **2010**, *10*, 2839.